STATIC FAILURE IN Al 2219-T87 PRESSURIZED VESSELS

by

E. S. Folias [1] and Phil Bogert [2]

[1] Department of Mathematics, University of Utah, Salt Lake City, Utah 84112

[2] Structural Mechanics Branch, NASA Langley Research Center, Hampton, Virginia 23681

ABSTRACT

Utilizing the theory of thin shell structures, a failure criterion is presented that one may use to predict, analytically, the critical crack length that may cause catastrophic failure, or unzipping, in cylindrical pressurized vessels, by knowing only the geometry and the material fracture toughness K. This fracture toughness K, may be obtained from tests data carried out on flat plates of the same material and thickness as that of the pressurized vessel and subjected to an equivalent type of loading. The test results, however, must be plotted as a function of the characteristic ratio (h / c), where h represents the specimen thickness and c one half the crack length. Comparison with carefully controlled experimental data substantiates its validity and its potential use.

The advantage of such an approach is that considerable amount of time and money may be saved for it is now possible to predict the response behavior of pressurized vessels from test data carried out on flat plates.

1. INTRODUCTION.

It is well known that large, thin-walled, pressurized vessels resemble balloons and like balloons are subject to puncture and explosive loss. For a given material, under a specified stress field due to an internal pressure q_o , there will be a crack length in the material which will be self-propagating. Crack lengths less than the critical value will cause leakage but not destruction. However, if the critical crack length is ever reached, either by penetration or by the growth of a small fatigue crack, explosion and complete loss of the structure may occur.

The principal task of fracture mechanics is precisely the prediction of such failures in the presence of sharp discontinuities, based on geometry, material properties, material behavior, and external loading. More specifically, the approach is based on a corollary of the first law of thermodynamics, that was first applied to the phenomenon of fracture by Griffith in 1924. His main hypothesis was that the total energy of a cracked system subjected to a loading remains constant as the crack extends an infinitesimal distance.

Griffith applied his criterion to the stretching of an infinite isotropic plate containing a flat, sharp-ended, crack of length 2c. Following similar lines, Folias (1970) derived a similar failure criterion for the prediction of failure in pressurized vessels by knowing only shell geometry, material properties, and loading. The purpose of this paper is basically twofold : (i) to clarify the proper interpretation and usage of the derived analytical criterion and (ii) to substantiate its validity and its potential use with carefully controlled experiments. Perhaps it may be appropriate here to note that, on a few previous occasions, the above criterion has been misused by some researchers in attempting to predict failure in pressurized vessels.

2. CORRELATION BETWEEN PRESSURIZED VESSELS AND FLAT PLATES.

Utilizing the theory of thin, shallow shells, Folias (1964, 1965) showed that, if one allows the radius R of a cylindrical pressurized vessel to tend to infinity, the hoop stress at failure, as a result of fracture, is related to the failing stress of a flat plate subjected to an equivalent type of loading through the equation

$$\frac{\sigma_{hoop}}{\sigma_{plate}} = \frac{1}{1+f(\lambda)} \quad , \qquad (1)$$

where $f(\lambda)$ is a geometric intrinsic property that, in the limit, as $R \rightarrow \infty$, tends to zero. Moreover, the parameter λ is defined by

$$\lambda^2 = \sqrt{12(1-\nu^2)}\,\frac{c^2}{Rh} \qquad (2)$$

where

R = the radius of the cylindrical vessel
h = the wall thickness

c = the half crack length
ν = Poisson's ratio

As a practical matter, eq. (1) correlates flat sheet behavior with that of initially curved specimens subjected to an equivalent loading. In experimental work on brittle fracture, for example, considerable time and money can be saved if one could predict the response behavior of curved sheets from test data carried out on flat plates of the same thickness. Equation (1) does precisely that.

3. ANALYSIS OF TESTS CARRIED OUT ON FLAT PLATES.

Tests on, cracked flat plates made of aluminum 2219-T87, were carried out by Royce Foreman (NASA) and the results can be found in Appendices A & B. These results may now be used to determine the fracture toughness, K, which, in conjunction with the theory developed by Folias (1974), may then be used to predict catastrophic failures in pressurized vessels. However, in order to accomplish this one must examine the available experimental data from a slightly different point of view.

It has long been recognized by the fracture community that the fracture toughness parameter is not a material constant, and that its true value depends strongly on the specimen thickness. The behavior is shown schematically in Fig.1. The reader will note that beyond a certain thickness h_s , a state of plane strain prevails and toughness reaches the so called plain strain value K_{Ic}. Alternatively, there exists an optimum thickness h_o , at which point toughness reaches its highest value. This level is usually referred to as plane stress fracture toughness with a failure that is characterized as shear or slant fracture. Moreover, for a thickness smaller than h_o there has been some uncertainty about the toughness. In some cases, a horizontal level was found (Allen 1971, Feddersen 1970), while in other cases a decreasing toughness was observed (Broek 1966, Christensen 1961, Weiss 1965). It may also be noted that for thicknesses below $h < h_o$, the plastic zone is approximately equal to the specimen thickness and yielding in the thickness direction is unconstrained. As a result, a state of plane stress can fully develop in such regions. Presently, it is widely accepted that for $h < h_o$ the fracture toughness decreases almost linearly to the value of zero. Experimental evidence of this, for 7075-T6 aluminum alloy, is shown in Fig. 2 (see Tetelman 1967, p. 136).

Additionally, recent, three-dimensional, analytical studies on flat plates carried out by Folias and his co-workers reveal that the stress concentration factor (1989, 1990), as well as the stress intensity factor (1975), are actually functions of the radius to half thickness ratio (a / h), and half crack size to half thickness ratio (c / h), respectively. For this reason, in Appendix C, we tabulate Foreman's experimental fracture toughness data as a function of the parameter (h / c), i.e. the thickness to half crack size ratio.

A careful examination of Appendices A, B & C reveal the following observations to be worthy of note:

(i) for the ratio of (h /c) = 0.047, the variation of the fracture toughness reported was approximately 12% !

(This is interesting particularly when the thickness, crack sizes and specimen widths were almost the same (see Appendix A, tests A). The variation suggests, perhaps, the presence of some sort of local material instability)

(ii) tests E, G, H do not appear to follow the expected trend. Something, apparently, was different in this set of experiments that the authors cannot speculate on and for this reason we will ignore (see Fig. 3)

(iii) tests 2J, 2K, 2L were carried out on flat plates with a 0.08 in. thickness and appear to be in line with the expected trend.

(iv) comparison between tests A & 2K show that, even though the ratio h / c is the same, and the ratio c / w is approximately the same, the values of the fracture toughness vary by 9%, which is in line with observation (i).

We conclude, therefore, that an experimental scatter of approximately 10 to 12 % is to be expected for this material.

4. THE FRACTURE TOUGHNESS CURVE.

Utilizing the data of the table in Appendix C, we now plot the experimental values of the fracture toughness K, as a function of the parameter (h / c) (see Fig. 3). The profile of the fracture toughness appears to follow the theoretically expected trend. Perhaps it is appropriate here to note that, this procedure works best if the experiments are carried out on flat plates of the same thickness. Unfortunately, the tests reported in Appendices A & B were carried out on flat plates with different thicknesses. Consequently, the reader may notice that tests A show a slightly higher rise than those of tests 2K. This occurs in the region which is characterized with a 45° plane fracture or more commonly referred to as *' shear fracture '*.

The reader may also notice that the thickness for the tests # A is h = 0.191 in. (see Appendix A), while the thickness for the test 2K is h = 0.083 in. (see Appendix B). This observation brings the following two questions to mind. Why is there a need for the presence of two different paths ? Moreover, at what value of h / c does this bifurcation take place ?

A partial answer to the above two questions may be obtained from the results of the work on the, 3D, stress field of a plate weakened by the presence of a circular hole (Folias et. al., 1990). Recently, utilizing a more sophisticated numerical analysis, the results have further been sharpened (Folias 1997) and the maximum, 3D, stress concentration factor versus the radius to half thickness ratio is shown in Fig. 4. The results of this figure provide us with a definite answer, at least for the case of a circular hole, of the regions in which a plate is considered to be in a state

of plane stress, i.e. a / h > 10, or in a state of plane strain, i.e. for a / h < 0.10. Moreover, the transition region occurs between the values of $0.10 < a / h < 10$, whereby the 3D effects become more pronounced. Thus, if one assumes that a similar trend also prevails in the case of a, 3D, cracked plate, one may conjecture that a state of plane stress exists for ratios of $h / c < 0.1$. This result appears to be in line with the experimental curves of Fig. 2 and Fig. 3. Furthermore, it is also known that for $h < h_o$, the fracture toughness is proportional to $\sqrt{h\varepsilon_f}$. As a result, it is not unusual to have a fan, or a series of paths, for different thicknesses that fan out to the left of the critical ratio $h / c = 0.1$. Such conjecture, may explain the experimental observations noted by researchers in the past (see discussion of Fig. 1).

5. FAILURE PREDICTION IN PRESSURIZED VESSELS.

The fracture toughness curve, as given by Fig. 3, may now be used to predict *the static* failing pressures in cylindrical vessels made of Al 2219-T87. For static considerations, the results by Folias (1974) should be applicable. More specifically, under the assumption that bending and bulging effects are negligible, Folias's general failure criterion (see Thin-Shell Structures, Chapter 21, editors Fung and Sechler, Prentice-Hall, 1974) may then be approximated by the simple relationship

$$\frac{q_o}{1000}\frac{R}{h}\sqrt{\pi c}\,\sqrt{1+0.317\lambda^2} = K \quad , \qquad (3)$$

where q_o is expressed in psi. Alternatively, if the effects of bending and bulging are sufficiently large, then the approximate eq.(3) can no longer be used and the general failure criterion must be utilized.

Recently, two very carefully controlled experiments on pressurized vessels were carried out by Nemat Nasser and his group at UCSD. The work was done in order to assess the structural characteristics of the United States Manned Module of the International Space Station. The tests were carried out on cylindrical pressurized vessels, of 20.75 in. in diameter and for two different values of thickness, $h = 0.05$ in. and $h = 0.086$ in. respectively. The cylinders were made out of Al 2219-T87.

A crack length of $2c = 5.5$ in. was very cleverly introduced by the rapid impact of a knife edge. The crack resembled a very sharp ellipse with crack tips sharp enough to represent a crack. Subsequently, the vessels were sealed internally with a thick hard rubber sheet, in the area of the crack, and were then pressurized incrementally with pressure differentials of 5 psi. This incremental 'pressure stepping' clearly suggests that the bending and bulging effects can no longer be neglected since they represent a cumulative effect.

Let us examine next, how well can one predict the failing pressures for the UCSD static tests # 1 & # 2. A closer examination of the geometrical and loading characteristics of test # 1 reveal that, because λ is greater than 5.5 and because the bending effects present are not

negligible, one must use the general failure criterion by including the pertinent bending terms which in this case are significant. In view of this, eq. (3) now becomes

$$\frac{q_o}{1000}\frac{R}{h}\sqrt{\pi c}\,F(\lambda) = K \quad , \qquad (4)$$

where $F(\lambda)$ is given numerically in the above reference. Without going into the numerical details (see Appendix D), the predicted results for tests # 1 and # 2 become respectively :

General Data :

$2R = 20.75$ in., $\qquad 2c = 5.5/2$ in.

(i) UCSD static test # 1 :

For test # 1, $h = 0.05$ in. and $h / c = 0.02$, and from Fig. 3 one reads a value of K that is closest to that thickness

for test # 1, using $K = K_{lower} = 62$ ksi$\sqrt{\text{in.}}$, $q_o = 31.2$ psi. $\qquad (5)$

The failing pressure reported was 34.4 psi.

It should, furthermore, be noted that for the UCSD test # 1, the hard rubber sheet used to seal the crack was well bonded to the interior surface of the vessel. Consequently, the rubber did carry some load and this was substantiated after the failure since it fractured along the same direction of the crack and at a 45^0 plane through its thickness. In carrying out test # 2, however, the rubber sheet was not bonded to the vessel. We have estimated the load carrying capacity of the rubber sheet for test # 1 to be approximately 1.6 psi. Thus, accounting for the rubber (see Appendix E), we predict a failing pressure for test # 1 to be, approximately, 32.8 psi.

(ii) UCSD static test # 2 :

For test # 2, $h = 0.086$ in. and $h / c = 0.03$, and from Fig. 3, one reads a value of K that is closest to that thickness

for test # 2, using $K = K_{lower} = 65$ ksi$\sqrt{\text{in.}}$, $q_o = 59.6$ psi. $\qquad (6)$

The failing pressure reported was 59.9 psi.

Perhaps it is appropriate here to emphasize that in both, UCSD, tests the upper and lower faces of the crack were not touching.

6. CONCLUSIONS.

In view of the foregoing analysis, the authors conclude that :

(i) Foreman's test data on cracked plates, as depicted in Fig. 3, are indeed very meaningful.

(ii) UCSD static tests # 1 & # 2 are compatible with Foreman's results and follow the theoretically expected curve.

(iii) Failure in cylindrical pressurized vessels can be predicted from tests data carried out on flat plates.

(iv) Plasticity effects present are negligible.

(v) UCSD tests data # 1 & # 2 depict a failure of plane stress or shear failure , i.e. 3D effects are negligible (except as they appear through the curve of the fracture toughness K, i.e. Fig. 3).

(vi) The US space station falls into the region of shear failure, i.e. the region to the left of the point $h / c = 0.08$ (see Fig.3), but with a value of $\lambda < 4$..

7. STATIC CRITICAL CRACK LENGTHS FOR THE US SPACE STATION.

Based on :

(i) Foreman's test data on cracked flat plates

(ii) UCSD static tests #1 & #2

(iii) the fracture toughness profile of material Al-2219-T87, as depicted in Fig. 3

the authors, after carrying out some further analysis, conclude that the *static critical crack length* for the US Manned Module of the International Space Station is :

(Assumed Data : R = 83 in., h = 0.190 in., K = 74 ksi$\sqrt{\text{in.}}$)

$$2c_{critical} = 16.4 \quad in.. \qquad (7)$$

It turns out that there are orbital debris impact scenarios that can produce crack sizes of this magnitude in the Space Station module. Although they are very rare and of very low measure of probability of its occurrence, nevertheless the subject warrants careful investigation of the possible risks to the astronauts on board.

8. REFERENCES

Allen, F. C., Effect of Thickness on the fracture toughness of 7075 aluminum in the T6 and T73 conditions, ASTM STP 486, (1971) pp. 16-38

Broek, D., The residual strength of light alloy sheets containing fatigue cracks, Aerospace Proceedings 1966, pp. 811-835, McMillan (1966)

Christensen, R. H. and Denke, P. H., Crack strength and crack propagation characteristics of high strength materials, ASD-TR-61-207 (1961)

Feddersen, C. E., et al., An experimental and theoretical investigation of plane stress fracture of 2024-T351 Al-alloy, Battelle Columbus rept. (1970)

Folias, E., S., 1965. An axial crack in a pressurized cylindrical shell. *Intern. J. Fracture Mech.* 1: 20-46.

Folias, E., S., 1974. Fracture in pressure vessels. *Thin Shell Structures*, Y. C. Fung and E. E. Sechler, editors, chapter. 21.

Folias, E. S. and Wang, J. J., On the 3D stress field in a plate weakened by a hole, International Journal of Computational Mechanics, 1990

Folias, E. S., Journal of Applied Mechanics, Vol. 42, No. 3 (1975), pp. 663-674.

Folias, E. S., Private communication.

Foreman, R., 1995. Private communication.

Griffith, A., A., 1924. The theory of rupture. *Proc. 1st Intern. Congr. on Appl. Mech.*, Delft, pp. 55-63.

Penado, F. E., and Folias, E. S., The 3D stress field around a cylindrical inclusion in a plate of arbitrary thickness, *Intern. J. Fracture Mech.* 39 (1989): pp.129-146.

Tetelman, A. S. and McEvily, A. J., Fracture of structural materials, John Wiley and Sons, Inc. 1967

Weiss, V. and Yukawa, S., Critical appraisal of fracture mechanics, ASTM STP 381, (1965) pp. 1-29

APPENDIX A

Summary of 2219-T87 Fracture Toughness K Experimental Test Data by Roy Foreman.

Spec. No.	Thick. h(in.)	Spec. Width W (in.)	Initial Crack 2c (in.)	Failure Stress (ksi.)	K (in.)
1A	0.19	20.05	8.11	18.52	73.69
2A	0.19	20.05	8.11	18.91	75.18
3A	0.19	20.04	8.07	20.04	79.29
4A	0.19	20.05	8.22	17.85	71.72
5A	0.19	20.05	8.11	17.92	71.29
1B	0.19	9.93	1.04	40.24	51.77
2B	0.19	10.03	1.04	39.78	53.68
3B	0.19	9.97	1.11	42.96	57.11
1C	0.19	10.04	2.15	33.11	62.53
2C	0.19	9.98	2.18	32.21	61.49
3C	0.19	9.98	2.17	32.86	62.48
1D	0.19	10.03	3.64	26.71	69.53
2D	0.19	9.98	3.65	25.41	66.41
3D	0.19	10.02	3.59	25.51	65.86
1E	0.19	9.98	5.13	17.96	61.26
2E	0.19	10.02	5.09	18.49	62.59
3E	0.19	10.04	5.12	18.91	64.24
1F	0.19	3.91	0.65	44.96	46.05
2F	0.19	3.91	0.64	46.01	47.01
3F	0.19	3.91	0.65	43.82	45.01
1G	0.19	3.91	1.16	35.01	49.94
2G	0.19	3.91	1.16	35.01	49.94
3G	0.19	3.91	1.18	35.62	51.36
1H	0.19	3.91	2.16	21.23	48.81
2H	0.19	3.91	2.17	21.29	48.95
3H	0.19	3.91	2.11	21.81	48.92

APPENDIX B

Spec. No.	Thick. h(in.)	Spec. Width W (in.)	Initial Crack 2c (in.)	Failure Stress (ksi.)	K (in.)
2J	0.08	10.06	2.08	29.71	68.52
2K	0.08	10.01	3.61	21.71	67.58
2L	0.08	10.01	5.08	14.61	60.19

APPENDIX C

FRACTURE TOUGHNESS
(Test Data by Roy Foreman)

test	h/c	K	2c/2w
A	0.05	74	0.41
B	0.34	54	0.11
C	0.18	62	0.22
D	0.1	67	0.36
E	0.08	63	0.51
F	0.6	46	0.16
G	0.33	51	0.3
H	0.18	49	0.56
2J	0.08	69	0.21
2K	0.05	68	0.36
2L	0.03	60	0.51

APPENDIX D

FAILURE CRITERION :

$$\sigma_{hoop}\sqrt{\pi c}\,\{f_e(\lambda) + f_b(\lambda)X(\lambda)\} = K \quad ; \ \lambda < 8. \qquad \text{(Eq. 1)}$$

where :

$$\lambda^2 = \sqrt{12(1-\nu^2)}\,(\frac{c^2}{Rh})$$

$$X(\lambda) = \frac{\sigma_{bending}}{\sigma_{hoop}} \doteq \frac{1}{6}\frac{\pi}{64}\lambda^2$$

For test # 1, $f_e(\lambda) = 4.00 - 0.12X(\lambda)$, $f_b(\lambda) = (-0.12 - 0.22X(\lambda))3.33$

For test # 2, $f_e(\lambda) = 3.21 - 0.11X(\lambda)$, $f_b = (0.02 - 0.23X(\lambda))3.33$

REMARK :

When no bending is present, the criterion may be approximated by the simple relation:

$$\sigma_{hoop}\sqrt{\pi c}\,\sqrt{1 + 0.317\lambda^2} = K \quad ; \ \lambda < 8. \qquad \text{(Eq. 2)}$$

REFERENCE :

Folias, E. S. 1974 " Thin Shell Structures " editors Y. C. Fung and E. E. Sechler, Prentice Hall

APPENDIX E

ESTIMATE OF LOAD CARRIED BY RUBBER SEAL.

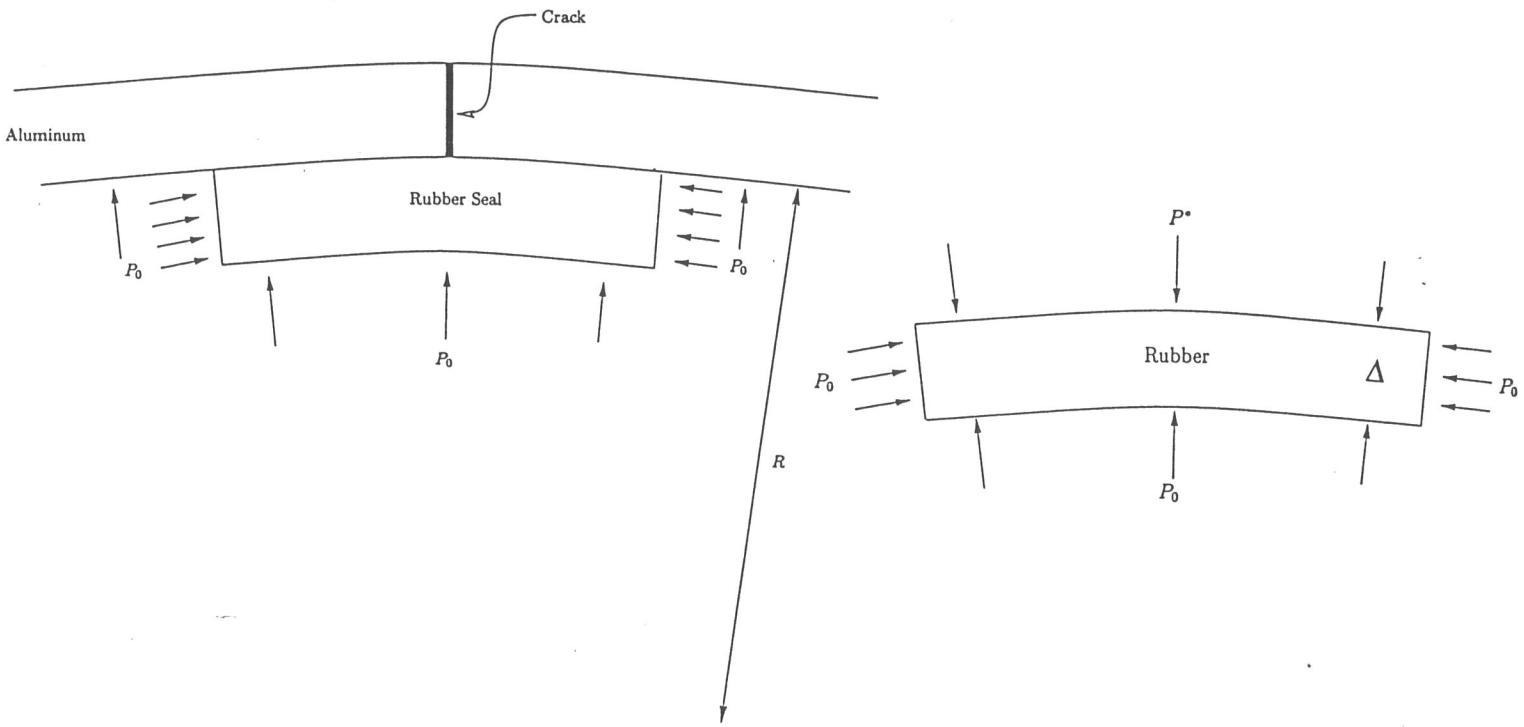

p_o = internal pressure

p^* = normal pressure between rubber and aluminum vessel

Equilibrium of rubber segment implies :

$$p_o - \frac{(p_o - p^*)(R-\Delta)}{\Delta} = 0 ,$$

or

$$p^* = (1 - \frac{2\Delta}{R})/(1 - \frac{\Delta}{R})p_o = (1 - \frac{\Delta}{R})p_o + O(\Delta^2)$$

For $\Delta = 0.50in.$, $R = 10.40in.$

$$p^* = (1 - \frac{0.50}{10.40})p_o = 0.95p_o ,$$

hence the aluminum vessel experiences, locally, a pressure equal to $0.95p_o$, and

$$p_{fail} = \frac{31.20}{0.95} = 32.80 \quad psi.$$

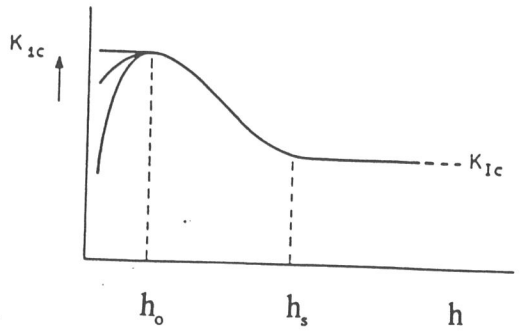

Fig. 1. Fracture toughness versus specimen thickness.

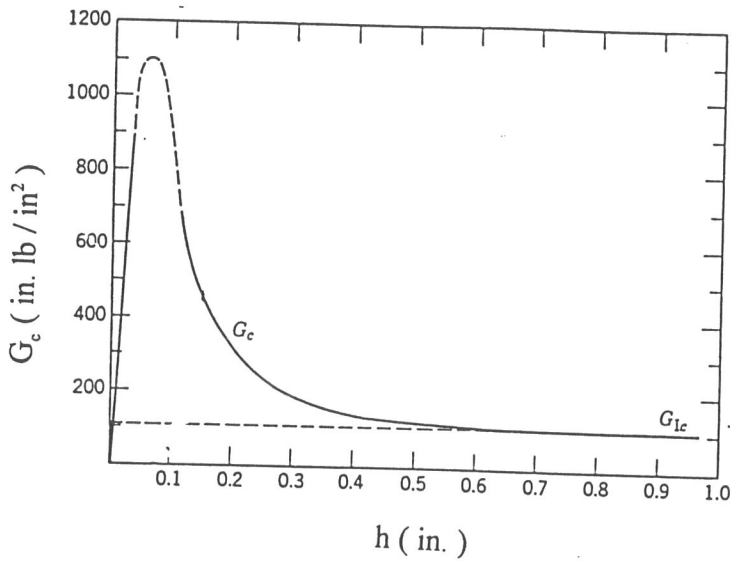

Fig. 2. Strain-energy release rate versus specimen thickness for 7075-T6 aluminum alloy.

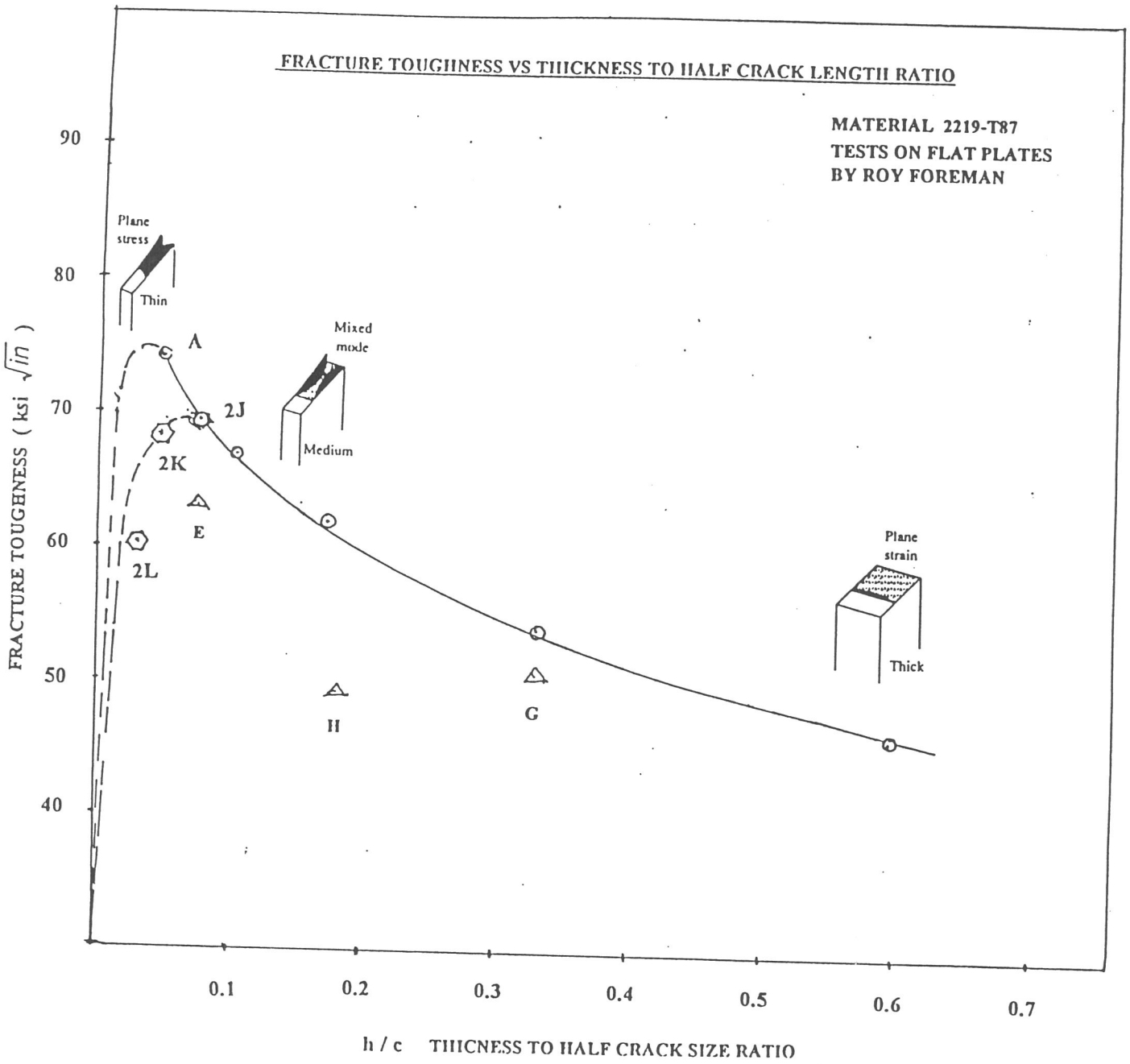

Fig. 3. Fracture toughness versus thickness to half crack length ratio for 2219-T87 aluminum alloy plates.

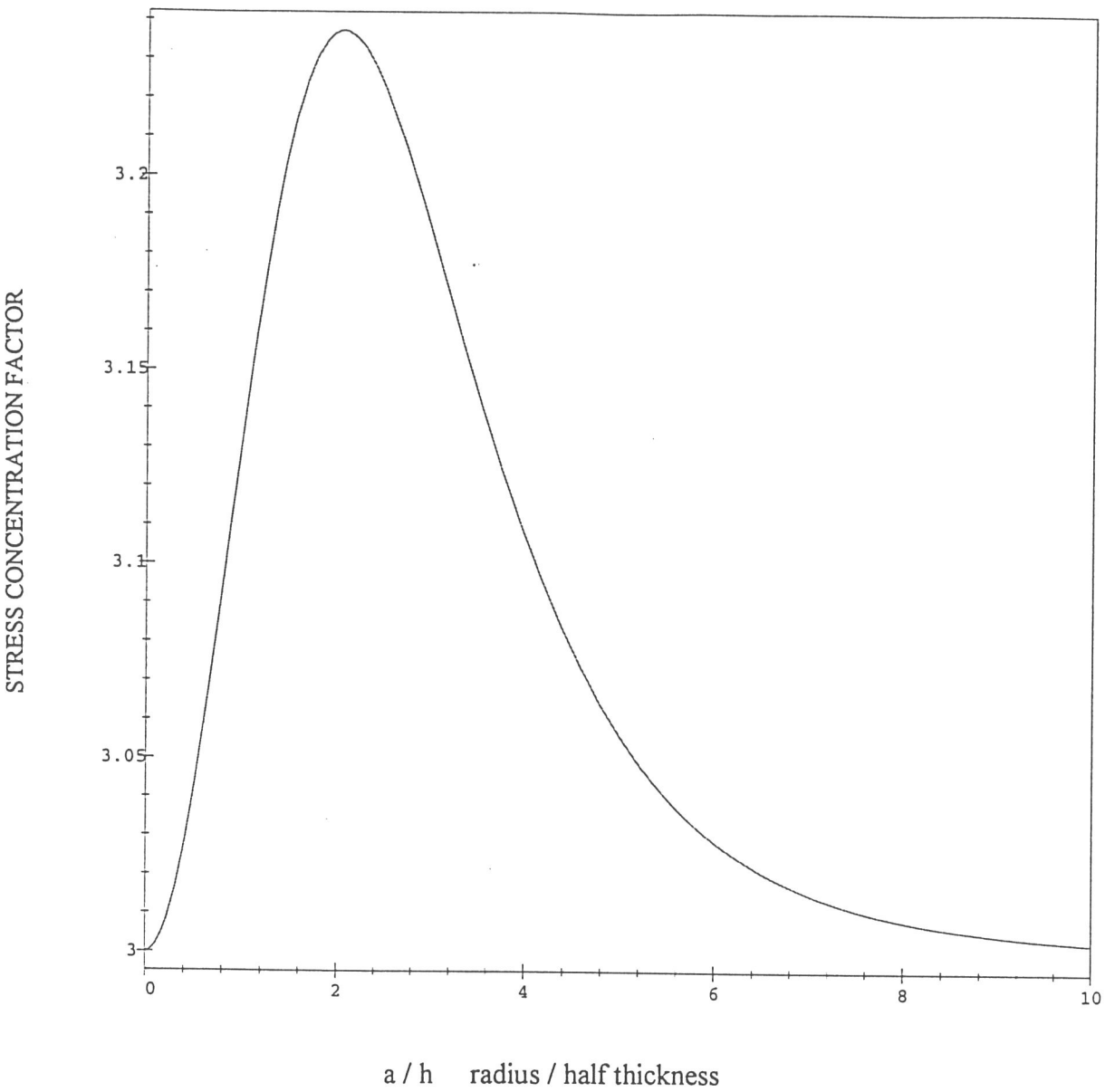

Fig. 4. Maximum stress concentration factor versus diameter to thickness ratio.